Murine Double Hit Model for Neonatal Cardiopulmonary Diseases: Bronchopulmonary Dysplasia (BPD) and Pulmonary Hypertension Associated with BPD

Steven P. Garrick[1, 2], Philip J. Berger[1, 2], Marcel F. Nold[1, 2, 3], and Claudia A. Nold-Petry[1, 2, *]

[1]Department of Paediatrics, Monash University, Melbourne, Victoria 3168, Australia
[2]Ritchie Centre, Hudson Institute of Medical Research, Melbourne, Victoria 3128, Australia
[3]Monash Newborn, Monash Children's Hospital, Melbourne, Victoria 3168, Australia
*For correspondence: claudia.nold@hudson.org.au

Abstract

Bronchopulmonary dysplasia (BPD) and pulmonary hypertension associated with BPD (BPD-PH) are of multifactorial origin and share common risk factors. Most murine models of BPD expose newborn pups to only one of these risk factors—more commonly postnatal hyperoxia—thereby mimicking the vital increased fraction of inspired oxygen (FiO_2) that preterm infants in neonatal intensive care units often require. To improve representation of the multifactorial origins of BPD and BPD-PH, we established a double hit model, combining antenatal systemic inflammation followed by postnatal hyperoxia. On embryonic day 14, pups are exposed to systemic maternal inflammation via a single intraperitoneal injection of 150 µg/kg of lipopolysaccharide to the dam. Within 24 h after birth, pups and dams are randomized and exposed to gas with either an FiO_2 of 0.21 (room air) or 0.65 (hyperoxia 65%). In our BPD and BPD-PH double hit model, we can obtain multiple readouts from individual pups that include echocardiography, lung histology and immunohistochemistry, ex vivo X-ray micro computed tomography, and pulmonary and plasmatic immunity by RNA, protein, or flow cytometry.

Graphical abstract
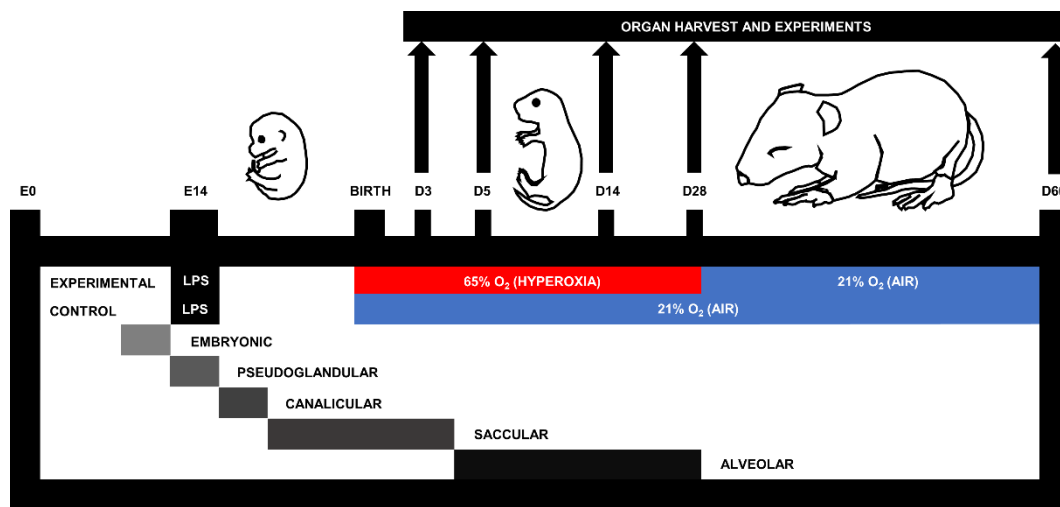
Figure 1. Murine double hit model of cardiopulmonary disease.
On embryonic day (E)14, pups are exposed to systemic maternal inflammation via a single intraperitoneal injection of 150 µg/kg lipopolysaccharide to the dam. Within 24 h after birth, pups and dams are randomized to be exposed to gas with either a fraction of inspired oxygen (FiO$_2$) of 0.21 (air; 21% O$_2$) or 0.65 (hyperoxia; 65% O$_2$) for a maximum of 28 days. According to the murine stage of lung development (Schittny, 2017), experimental endpoints include postnatal day (D)3, D5, D14, D28, and D60.

Background

Bronchopulmonary dysplasia (BPD) and pulmonary hypertension secondary to BPD (BPD-PH) are severe cardiopulmonary morbidities of premature infants that are underpinned by a surge in pulmonary inflammation. Pulmonary inflammation interrupts alveolar and vascular development, compromising gas exchange in infants with BPD (Thebaud et al., 2019). According to a systematic review and meta-analysis, approximately 17% of all infants with BPD develop BPD-PH, with a mortality rate of 14%–38% (Al-Ghanem et al., 2017). BPD-PH occurs due to a reduced cross-sectional area of the pulmonary vasculature that increases pulmonary vascular resistance and hence blood pressure (Parker and Abman, 2003; Khemani et al., 2007).

   Pulmonary inflammation in the preterm infant can originate from many sources, with maternal inflammation being particularly prominent (Kemp, 2014). Environmental factors (stress, alcohol, smoking), autoimmune conditions (lupus erythematosus, inflammatory bowel disease, diabetes), and inflammatory pregnancy conditions (preeclampsia, chorioamnionitis) all contribute to a pro-inflammatory uterine environment in the mother. Infants with chorioamnionitis present with increased umbilical serum levels of pro-inflammatory cytokines including IL-1β, IL-6, and TNF (Dollner et al., 2002), which are important malefactors in BPD and BPD-PH (Sahni et al., 2020). Systemic maternal inflammation can be simulated in mice with an intraperitoneal (i.p.) injection of lipopolysaccharide (LPS), a bacterial endotoxin that binds to the toll-like receptor 4, a pattern recognition receptor of the innate immune system that promotes expression of pro-inflammatory cytokines, including IL-1β, TNF, and IL-6 (Palsson-McDermott and O'Neill, 2004). In pregnant rats, i.p. injection of 2.5 mg/kg LPS at gestational day 20 and 21 (full term = 22 days) resulted in prolonged pulmonary inflammation and delayed lung maturation in the offspring (Cao et al., 2009).

   Unfortunately, early life inflammation is perpetuated postnatally by lifesaving interventions received in the neonatal intensive care unit. The most prevalent is the use of an increased fraction of inspired oxygen (FiO$_2$) (hyperoxia) delivered to the preterm infant to counteract the reduced diffusing capacity of the immature lung. Although hyperoxia saves the life of the infant, it also comes with the unfortunate consequence of increased

pulmonary inflammation via the production of reactive oxygen species (Torres-Cuevas et al., 2017).

Mimicking multifactorial diseases by including multiple pathophysiological drivers into in vivo models will lead to greater methodological rigor for translation transition of lifesaving therapies into clinics. However, to date, many murine BPD models only use one insult, namely hyperoxia. At the time we introduced our model, to the best of our knowledge, double hit strategies had been applied only twice to mimic BPD in newborn rodents (Choi et al., 2009; Velten et al., 2010), whereas there was none established to assess BPD-PH. Choi et al. (2009) first recognized the relevance of a double hit model, discovering that intra-amniotic LPS (0.5 or 1.0 mg) administration at day 20 of gestation (full term = 22.5) in neonatal rats amplified the lung injury induced by one week of exposure to hyperoxia (85% O_2). One year later, Velten et al. (2010) injected 80 µg/kg LPS (i.p.) to pregnant mice at day 16 of gestation (full term = 19-21); upon birth, they placed pups in hyperoxia (85% O_2) for 14 days followed by room air for another 14 days. These pups presented with a phenotype of arrested alveolarization, diffuse fibrosis, and impaired lung mechanics.

Expanding on these BPD models, we set out to establish a murine double hit model of early life cardiopulmonary disease representative for BPD and BPD-PH (Nold et al., 2013) (**Figure 1**). First, dams are injected (i.p.) with 150 µg/kg of lipopolysaccharide on day 14 of gestation, and upon birth pups are subsequently placed in hyperoxia (65% O_2) or housed under room air control conditions. Pups subjected to this double hit develop alveolar and vascular changes representative of clinical features in BPD and BPD-PH. Our double hit model distinguishes itself from the earlier combined models by minimizing the FiO_2 (65% compared to 85%) to better reflect clinical practice. Intuitively, we hypothesized that any improvement in BPD would most likely also improve BPD-PH, because of the inextricable link between alveolarization and angiogenesis.

Our team has established an experimental endpoint protocol so we could simultaneously investigate combinations of multiple individual readouts from every individual pup, including ex vivo (lung histology, immunohistochemistry, flow cytometry, x-ray micro computed tomography, precision cut lung slices, pulmonary/plasmatic immunity) and in vivo readouts (cine-angiography, echocardiography). Plethysmography, behavioral changes, and long-term neurodevelopmental outcomes could be considered as additional in vivo outcomes.

Our discovery that neonatal cardiopulmonary disease is underpinned by type 2 immunity (Lao et al., 2022) confirmed a pathogenetic similarity between BPD and asthma that has been speculated (de Kleer et al., 2016) but never fully proven. Proof of concept from our murine BPD/PH model (**Figure 1**) in a STAT6 deficient mouse, which lacks a full type 2 immune response, confirmed that the type 2 pathway is critical to the pathophysiology of BPD/PH and that blockade of type 2 pathways is highly effective in preventing the disease. This revelation might shift the current paradigm for treating BPD, which relies on gentle ventilation techniques and, ultimately, the use of corticosteroids as a rescue therapy. In the future, seeing BPD and BPD-PH as a type 2 disease will open up the use of well tolerated anti-type 2 drugs as a novel treatment strategy. In addition, our preclinical studies, in which we apply our model and other early life disease models, have shown that early and effectively blocking inflammation, specifically the potent pro-inflammatory interleukin (IL)-1, also holds great promise for preventing BPD and BPD-PH (Nold et al., 2013; Royce et al., 2016; Bui et al., 2019). Blocking IL-1 using its natural adversary IL-1 receptor antagonist (IL-1Ra, drug name anakinra) has an excellent safety and efficacy record, which has been established over two decades via anakinra's clinical use in adults, children, and infants, as treatment for neonatal onset multi-system inflammatory disease (Sibley et al., 2012).

Materials and Reagents

1. Ultra-fine 31G insulin syringes 0.5 mL (Becton Dickinson, catalog number: 32281)
2. Insyte™ Autoguard™ winged, 24G × 0.75" (Becton Dickinson, catalog number: 381212)
3. Microlance™ hypodermic needle 30G × 0.5 (Becton Dickinson, catalog number: 304000)
4. 10 µL gastight syringe, cemented needle, 26s gauge, 2 in., point style 2 (Hamilton, catalog number: 1701)
5. C57BL/6J mice
6. Lipopolysaccharide (LPS) from *Escherichia coli* O127:B8; purified by phenol extraction (Sigma, catalog number: L3129)
7. Sodium chloride intravenous infusion BP (water for injection) (Pfizer, catalog number: AUST R 49280)
8. Oxygen gas

9. Isoflurane (AbbVie, Forthane®, catalog number: AUST R 29656, store below 30 °C)
10. Paraformaldehyde (PFA) powder, 95% (Sigma-Aldrich, catalog number: 158127)
11. PBS (ThermoFisher Scientific, Gibco™, catalog number: 14190250)
12. Cotton tip applicators (BSN Medical, catalog number: 7505-0)
13. Gauze
14. Liquid nitrogen (N_2)
15. Wet ice
16. Polyester thread (sutures) (Birch, catalog number: 004601)
17. 1.7 mL microtubules (Axygen, catalogue number: MCT-175-C)

Equipment

1. Custom plexiglass gas chamber [approximate dimensions: $40 \times 125 \times 30$ (L × W × H) cm]
2. Bear cub BP2001 infant ventilator (Bear Medical Systems, Type #240)
3. Portable oxygen analyzer (Teledyne, model: AX300-I)
4. Oxygen sensor (Maxtec, model: R109P09)
5. Power lab/16SP (ADinstruments, model: ML795)
6. Heated respiratory humidifiers (Fisher and Paykel, model: MR730)
7. Autofill humification chamber (Fisher and Paykel, model: MR290)
8. Temperature pod (ADinstruments, model: ML312)
9. Pod expander (ADinstruments, model: ML305)
10. Compact scale, 510 g × 0.1 g (A&D Weighing, model: HT-500)
11. Gravity perfusion apparatus
12. Forceps, tip width 0.5 mm, length 10 cm (Fine Science Tools, catalog number: 11150-10)
13. Scissors (Precision Medical Specialties, model: E25-500)
14. Foam dissection tray
15. Liquid nitrogen container (Nalgene®, catalog number: 4150-2000)
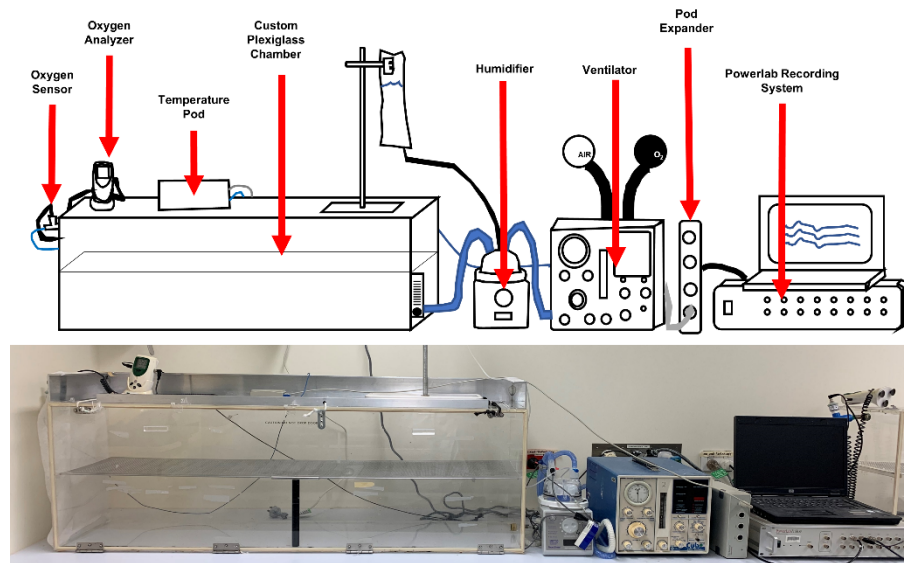16. -86 °C freezer 690 L (Froilabo, model: BMEVO69086G)

Software

1. Chart 5 Pro v5.5.1 (ADInstruments, www.ADInstruments.com)

Procedure

Murine double hit model of cardiopulmonary disease

A. Experimental conditions (Figure 2)

Figure 2. Setup of an experimental chamber.
A custom plexiglass chamber is connected to a humidifier and ventilator. Humidified oxygen gas with a fraction of inspired oxygen (FiO$_2$) of 0.65 is passed through the hyperoxia chamber at a flow rate of 10 L/min (air chamber has a FiO$_2$ of 0.21). Power lab recording system records temperature, humidity, and oxygen levels in chambers. Humidity and temperature are kept constant at 50%–60% and 22 °C, respectively. Light is cycled in a 12 h day/night rhythm. Chamber setup included below the schematic for comparison.

B. Time mating

1. Use C57BL/6J mice.
2. Breeders are housed in enhanced specific pathogen free 2 conditions.
3. Preparation of female breeders:
   a. Select 6–14-week-old females for consideration.
      i. Younger females might not be sexually mature.
      ii. Older females mate less reliably.
   b. One to two weeks prior to timed mating, house females together.
      Group housed females to synchronize their estrous cycles. This phenomenon is known as the "Lee-Boot effect" (Van Der Lee and Boot, 1955).
   c. Three days prior to timed mating, place material from a stud male cage into the female cages.
      The exposure of group housed female mice to urine from a male mouse increases the chance of ovulation on the third night following exposure. This phenomenon is known as the "Whitten effect" (Whitten, 1956).
4. Preparation of male breeders:
   a. Select 6–14-week-old males.
      Preference proved stud males as sexual experience improves male reproductive performance (Swaney et al., 2012).
   b. One to two weeks prior to timed mating, separate the stud males.
      This allows the sperm count to increase and libido to recover from any previous mating.
5. Timed mating:
   a. Place 1–2 females together with a stud male in a cage.
   b. Check for viscous vaginal plugs in the mornings.
      i. Components of the male ejaculate coagulate to form a hard plug that blocks the opening of the vagina and is an indicator of copulation. However, 37.1% of females that plug do not become pregnant (Heyne et al., 2015).

      ii.   A positive plug is considered embryonic age (E)0.5 if pregnancy occurs.

   c.   After 48 h together, separate breeding pairs.

C. Early pregnancy detection

1. Monitor body weight gain of females.
   Pregnant mice gain on average 3.49 g from E0 to E7–10 (Heyne et al., 2015).
Or
2. Palpate the pregnant dam's abdomen with the thumb and forefinger at E12.
   A positive pregnancy feels like a string of beads.

D. Antenatal inflammatory hit 1 at E14

1. Intraperitoneal injection of lipopolysaccharide (LPS) to the dam:
   a. Determine the dam's body weight.
   b. Prepare LPS injection.
      ii. Reconstitute LPS powder in water for injection.
      iii. Final concentration injected is 150 µg/kg.
      iv. Final volume injected is 1 µL/g.
   c. Inject LPS into the lower right quadrant of the dam at a 45° angle with an insulin syringe (**Figure 3**). Adverse events associated with i.p. injection are related to errors in the placement of the injection. Ensure that the needle passes through the skin, muscle, and peritoneum of the abdomen without penetrating any abdominal organs.
   d. Monitor dams closely to ensure welfare of animals.
   If miscarriage occurs, humanely euthanize the dam and perform a postmortem.
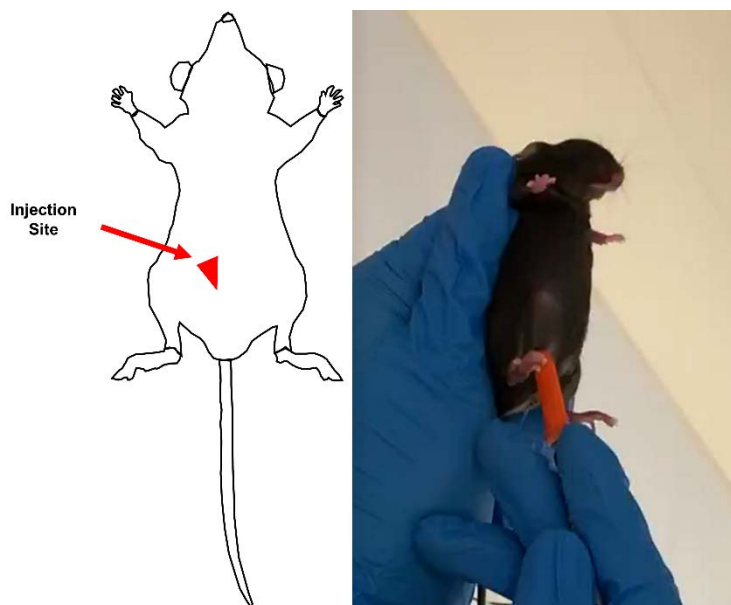
Figure 3. Intraperitoneal injection site for LPS on day 14 of gestation in the pregnant dam

E. Postnatal inflammatory hit 2

1. Dams deliver pups naturally at E19–21 in the saccular stage of lung development (Backstrom et al., 2011).

2. The saccular stage is most susceptible to lung injury in mice (Backstrom et al., 2011), comparable to a premature human baby at 24–38 weeks gestation (Swaney et al., 2012).
3. Within 24 h of birth, randomly assign pups and dams to either:
   a. Hyperoxia (FiO$_2$ of 0.65)
      Develop cardiopulmonary disease
   b. Normal room air (FiO$_2$ of 0.21)
      Control animals
4. Set up foster pairs to avoid oxygen toxicity in the dam; pair one dam with pups in a hyperoxia cage with a counterpart dam and pups in an air cage.
   In case of an odd number of deliveries:
   a. Allocate the extra dam to an air group.
      Or
   b. Distribute the pups from the extra litter into the other litters under the experiment.
5. Choose experimental endpoints to determine different readouts.
   a. Three days of 65% hyperoxia
      Pulmonary immunity:
      Postnatal exposure of pups to hyperoxia induces an immediate IL-1 and type 2 cytokine pulmonary immune response, which is most evident within the first three days of life. Accordingly, we see increased pulmonary IL-1β (20-fold), IL-1 receptor antagonist (2-fold) (Nold et al., 2013; Rudloff et al., 2017) type 2 cytokines (IL-4, IL-5, IL-13) (4- to 53-fold), and type 2 chemokines (CCL1, CCL17) (11- to 31-fold) (Lao et al., 2022).
   b. Five days of 65% hyperoxia
      i. Pulmonary immunity
         Transcription factors that regulate the development of all innate lymphoid cells (ILCs) (*Plzf* and *Id2*) and ILC2s (*Tcf7* and *Bcl11b*) are up to 23% lower after hyperoxia (Lao et al., 2022). There is a 2-fold increase in type 2 helper (TH2) cells after hyperoxia (Lao et al., 2022).
      ii. Pulmonary angiogenesis
         Hyperoxia elevates vascular endothelial growth factor by 1.4-fold and endothelin-1 by 1.4-fold in murine lungs (Bui et al., 2019).
   c. Fourteen days of 65% hyperoxia
      i. Alveoli
         Early changes in alveolar structure (Nold et al., 2013).
   d. Twenty-eight days of 65% hyperoxia
      i. Structural changes
         1). Alveoli
         Twenty-eight days marks the end of the alveolar stage of lung development in the mouse, similar to 2–3 years of age in humans (Backstrom et al., 2011). Hyperoxia reduces alveolar number (25%–44%), increases alveolar size (40%–230%), and reduces surface/volume ratio (18%–35%) (**Figure 4**) (Nold et al., 2013; Royce et al., 2016; Rudloff et al., 2017). These emphysematous changes in alveoli impair lung function by reducing the diffusing capacity of the lung (Pellegrino et al., 2005)
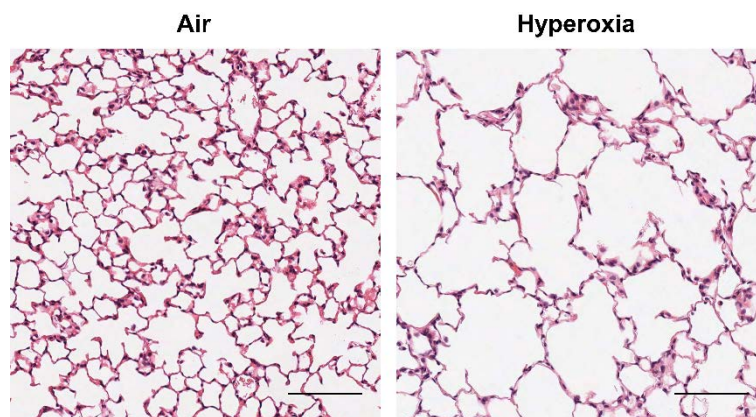
Figure 4. Emphysematous changes in lung morphology (H&E staining) at 28 days of life after antenatal LPS and postnatal exposure to 65% hyperoxia compared to air controls in C57BL/6J mice (sourced from Rudloff et al., 2017).
Scale bars 100 µm, ×200 magnification.

2). Airways
Hyperoxia increases airway epithelial thickness (25%), subepithelial collagen deposition (200%), expression of α-smooth muscle actin (50%), and expression of the proliferation marker cyclin D1 mRNA (260%) (Royce et al., 2016). However, hyperoxia does not alter the airway goblet cell mucus production (Royce et al., 2016).

3). Pulmonary vascular bed
Hyperoxia reduces the number of small vessels (4–5 µm diameter) (84%) (Bui et al., 2019; Lao et al., 2022). No differences in the expression of α-smooth muscle actin and endothelin receptor type-A after hyperoxia (Bui et al., 2019).

4). Heart
Hyperoxia increases cardiac fibrosis (2.2-fold) and fibrotic/inflammatory markers galectin-3 and CCL2 (C-C motif) (Bui et al., 2019).

5). Brain
Hyperoxia does not cause apoptosis, cortical neuronal lamination, temporal cortical width (at hippocampus), white matter myelination, hemorrhage, loss of neurons, gliosis, inflammation, or any other significant morphologic abnormalities in C57Bl/6J mice (Rudloff et al., 2017).

ii.   Functional changes
1). In vivo
The inversely related surrogate marker time to peak velocity/right ventricular ejection time, as measured by echocardiography, increases in hyperoxic pups (0.27 compared to 0.32 in air controls) (Bui et al., 2019; Lao et al., 2022).

2). Ex vivo
Hyperoxia increases luminal contraction of airways to the muscarinic acetylcholine receptor agonist methacholine (10–3,000 nM) (89%) compared to air (44%) in precision cut lung slices (Royce et al., 2016). Pulmonary arterial contraction to the vasoconstrictors endothelin 1 and U46619 is not altered by hyperoxia in precision cut lung slices (Bui et al., 2019).

iii.   Cellular immunity of the lung
After hyperoxia, the overall number of immune cells (neutrophils, lymphocytes, monocytes/macrophages, natural killer cells, and dendritic cells) is approximately 3.1-fold lower. However, increased activation of macrophages and dendritic cells, as well as elevated IL-1β, is still evident in the lungs (Nold et al., 2013).

e.   Sixty days (28 days hyperoxia, followed by 32 days room air)
Hyperoxia reduces vessel numbers at each branching generation in the murine lung (-18% in generation 2 and -21% in generation 3) (Bui et al., 2019).

F. Maintain comprehensive experimental records

1. Record oxygen application, temperature, and humidity with power lab instrument and Chart 5 Pro software.
2. Record assessments of animal welfare.

G. Fostering of pups (Figure 5 and Video 1)

Adult mice are more susceptible to hyperoxia-induced oxygen toxicity than neonatal mice (Frank et al., 1978). Therefore, dams need to be rotated between room air and hyperoxia pups in a three-day cycle to limit hyperoxia-induced toxicity. It is important to conduct this procedure promptly, so that pups are in the experimental conditions for as long as possible. Top up food and water during this step to minimize unnecessary opening of the hyperoxia chamber.

1. Remove cages from air and hyperoxia chambers.
2. Take one pair of one hyperoxia and one air cage at a time.
    a. Swap the pups between the paired dams
        i.   Air pups will be moved into the dam's cage that was previously in hyperoxia.
        ii. Hyperoxia pups will be moved into the dam's cage that was previously in air.
    b. Cover the pups in bedding material from the new cage
        i.   This procedure masks the scent of the other dam.
        ii. This reduces the likelihood of rejection from the foster dam.
    c. Repeat for all paired cages
3. Return cages to air and hyperoxia chambers.
    a. Pups are in the same conditions.
    b. Dams previously in hyperoxia chamber are now housed in the air chamber; however, the pups stay under their allocated experimental condition.
    c. Dams previously in air chamber are now housed in the hyperoxia chamber; however, the pups stay under their allocated experimental condition.
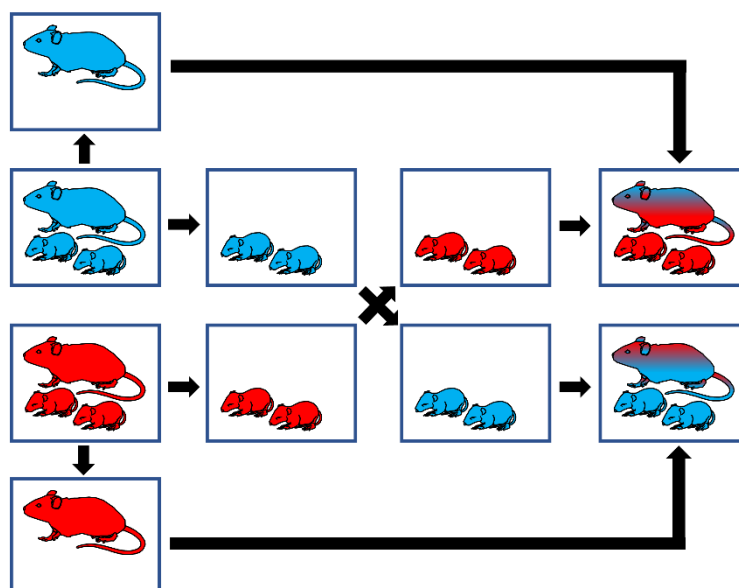
Figure 5. Fostering of pups.
Hyperoxia animals (red), air animals (blue). Air dam rotates into the hyperoxic chamber every three days. Hyperoxia dam rotates into the air chamber every three days. Pups are cross fostered every three days between
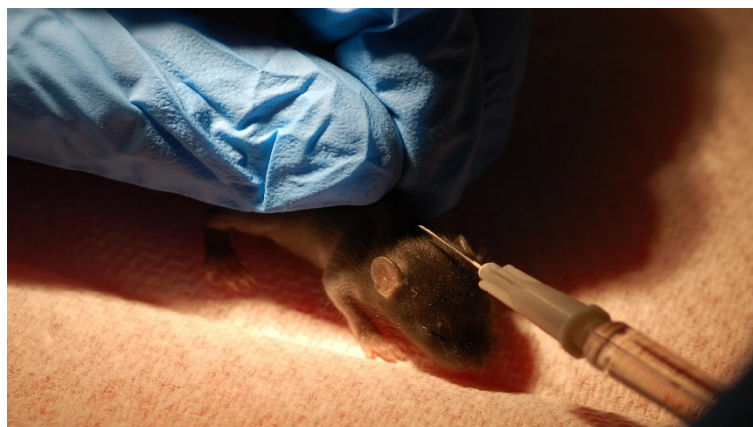
dams and, as a result, they are continuously housed under the same experimental condition from day 1.

Video 1. Fostering of pups

H. Subcutaneous injections of neonatal pups (Figure 6)

1. Gently scruff the pups.
    Lift the skin above the neck.
2. Insert the syringe at a 45° angle.
3. Inject pups slowly.
4. Pull out the needle slowly to prevent leakage.

Figure 6. Subcutaneous injection of 11-day-old C57BL/6J pup

## I. Sample preparation for lung histology and pulmonary immunity of a 28-day-old pup

1. Anesthetize the pup with isoflurane per open-drop method (Risling et al., 2012).
2. Euthanize the pup
    a. Cervical dislocation
        i.   Place the thumb and forefinger in between the head and neck of the animal.
             Note: The spinal column should be palpable.
        ii. Pinch the thumb and forefinger together and push down simultaneously until the cervical spine
             is cleanly separated.

1). Ensure that you do not apply too much pressure as the trachea needs to be intact for later inflation of the lung.

2). Pinch the foot with the forceps to ensure mouse is dead before dissecting.

3. Dissection (**Figure 7**, **Figure 8,** and **Video 2**)

    a. Pin the mouse on a foam dissection board on its back with its four limbs spread out.

    b. Hook the front teeth of the mouse with a suture; then, pull tight and pin to foam board.

       This procedure helps to straighten the trachea to allow better inflation.

    c. Dissect the mouse

       i. Cut through the ventral surface of the mouse from the sternum up to the chin.

       ii. Open the chest cavity such that the entire lung is visible.

       iii. Expose the trachea.

          1). The trachea is enclosed by the thyroid.

          2). Grasp the thyroid with forceps and pull apart to remove.

          3). Wipe away any excess blood with gauze soaked in PBS or use a cotton tip applicator.

          4). Delicately cut away tissue around trachea so that the forceps can reach underneath.

          5). Place two strings of suture underneath the trachea.

    d. Samples for pulmonary immunity

       i. Ensure that the left lobe is clearly visible.

       ii. Loop a piece of suture around the left lobe of the lung by holding the suture with your forceps and lift the lobe with a cotton tip applicator.

         Organ will stick to the cotton without being ripped or damaged. Lungs exposed to hyperoxia are fragile.

       iii. Now loop the suture around the left bronchus and tie the left lobe off.

       iv. Ensure knots are tight so that no leakage occurs during the right lung inflation.

       v. Cut off the left tied lobe, cut in two, and place in separate labeled 1.7 mL microtubules. Immediately snap freeze in liquid N_2 (following all safety protocols of your institution) for later mRNA and protein analysis.

         Store at -80 °C until ready for processing.

    e. Inflation of the right lung lobes

       i. Insert a 24G cannula into the trachea.

       ii. Tie the cannula in place with one of the sutures threaded earlier underneath the trachea.

       iii. Attach the cannula to a gravity perfusion apparatus.

       iv. Infuse the right lung lobes with 4% PFA (pH 7.4) under constant 20 cm H_2O of hydrostatic pressure.

         1). Reconstitute PFA powder with PBS.

         2). Full inflation is determined by the tip of the post-caval lobe turning pointy.

       v. Tie off the trachea with the second suture in front of the cannula to prevent backflow of PFA.

       vi. Place pup on ice for 10 min.

    f. Samples for histology

       i. Remove right lung lobes from thorax and place in tube with 4% PFA.

       ii. Keep in 4% PFA for a minimum of 6 h.

   iii. Process for paraffin embedding and sectioning.
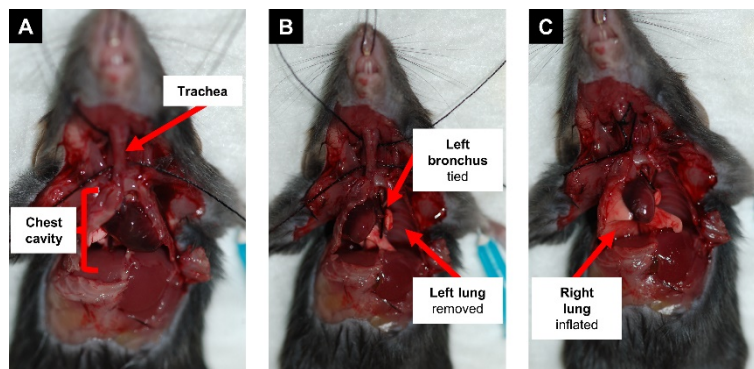
Figure 7. Sample preparation of a 28-day-old mouse.
Dissect the mouse and open the chest cavity to expose lungs and trachea (A). Tie off the left bronchus and remove the left lung for later analysis of pulmonary immunity (B). Inflate the right lung lobes with 4% paraformaldehyde for histology (C).
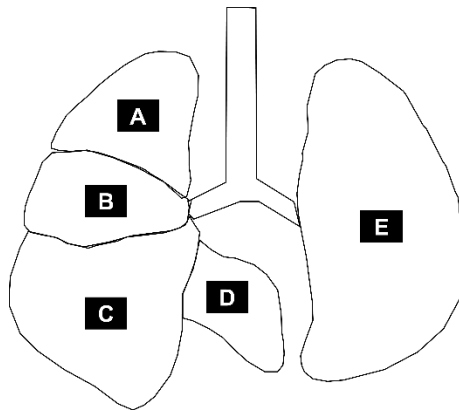
Figure 8. Pulmonary anatomy of a mouse.
The left lobe (E) and the right lobes [superior lobe (A), middle lobe (B), inferior lobe (C), and post-caval lobe (D)]. At day 28, the left lobe is removed for analysis of pulmonary immunity (top third for RNA, bottom two thirds for protein). The right lobes are subsequently inflated with 4% paraformaldehyde and sections for histology are made from the inferior lobe.
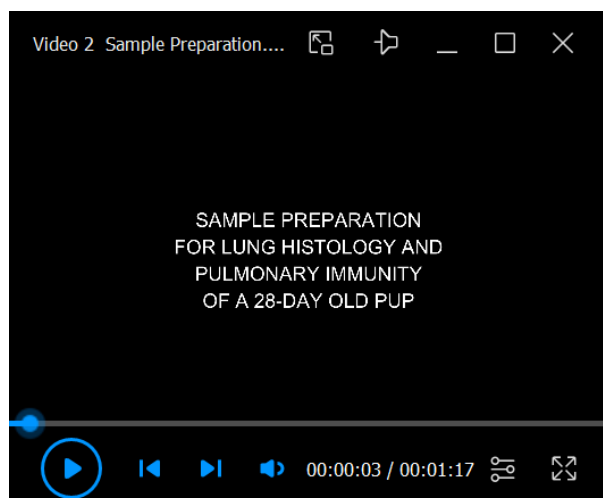
Video 2. **Sample preparation for lung histology and pulmonary immunity of a 28-day-old mouse**

Acknowledgments

Competing interests

The authors declare no competing interests.

Ethics

The double hit model protocol was approved by the animal review board MMCA of Monash University.

References

Al-Ghanem, G., Shah, P., Thomas, S., Banfield, L., El Helou, S., Fusch, C. and Mukerji, A. (2017). Bronchopulmonary dysplasia and pulmonary hypertension: a meta-analysis. *J Perinatol* 37(4): 414-419.

Backstrom, E., Hogmalm, A., Lappalainen, U. and Bry, K. (2011). Developmental stage is a major determinant of lung injury in a murine model of bronchopulmonary dysplasia. *Pediatr Res* 69(4): 312-318.

Bui, C. B., Kolodziej, M., Lamanna, E., Elgass, K., Sehgal, A., Rudloff, I., Schwenke, D. O., Tsuchimochi, H., Kroon, M., Cho, S. X., et al. (2019). Interleukin-1 Receptor Antagonist Protects Newborn Mice Against Pulmonary Hypertension. *Front Immunol* 10: 1480.

Cao, L., Wang, J., Tseu, I., Luo, D. and Post, M. (2009). Maternal exposure to endotoxin delays alveolarization during postnatal rat lung development. *Am J Physiol Lung Cell Mol Physiol* 296(5): L726-737.

Choi, C. W., Kim, B. I., Hong, J. S., Kim, E. K., Kim, H. S. and Choi, J. H. (2009). Bronchopulmonary dysplasia in a rat model induced by intra-amniotic inflammation and postnatal hyperoxia: morphometric aspects. *Pediatr Res* 65(3): 323-327.

de Kleer, I. M., Kool, M., de Bruijn, M. J., Willart, M., van Moorleghem, J., Schuijs, M. J., Plantinga, M., Beyaert, R., Hams, E., Fallon, P. G., et al. (2016). Perinatal Activation of the Interleukin-33 Pathway Promotes Type 2 Immunity in the Developing Lung. *Immunity* 45(6): 1285-1298.

Dollner, H., Vatten, L., Halgunset, J., Rahimipoor, S. and Austgulen, R. (2002). Histologic chorioamnionitis and umbilical serum levels of pro-inflammatory cytokines and cytokine inhibitors. *BJOG* 109(5): 534-539.

Frank, L., Bucher, J. R. and Roberts, R. J. (1978). Oxygen toxicity in neonatal and adult animals of various species. *J Appl Physiol Respir Environ Exerc Physiol* 45(5): 699-704.

Heyne, G. W., Plisch, E. H., Melberg, C. G., Sandgren, E. P., Peter, J. A. and Lipinski, R. J. (2015). A Simple and Reliable Method for Early Pregnancy Detection in Inbred Mice. *J Am Assoc Lab Anim Sci* 54(4): 368-371.

Kemp, M. W. (2014). Preterm birth, intrauterine infection, and fetal inflammation. *Front Immunol* 5: 574.

Khemani, E., McElhinney, D. B., Rhein, L., Andrade, O., Lacro, R. V., Thomas, K. C. and Mullen, M. P. (2007). Pulmonary artery hypertension in formerly premature infants with bronchopulmonary dysplasia: clinical features and outcomes in the surfactant era. *Pediatrics* 120(6): 1260-1269.

Lao, J. C., Bui, C. B., Pang, M. A., Cho, S. X., Rudloff, I., Elgass, K., Schroder, J., Maksimenko, A., Mangan, N. E., Starkey, M. R., et al. (2022). Type 2 immune polarization is associated with cardiopulmonary disease in preterm infants. *Sci Transl Med* 14(639): eaaz8454.

Nold, M. F., Mangan, N. E., Rudloff, I., Cho, S. X., Shariatian, N., Samarasinghe, T. D., Skuza, E. M., Pedersen, J., Veldman, A., Berger, P. J., et al. (2013). Interleukin-1 receptor antagonist prevents murine bronchopulmonary dysplasia induced by perinatal inflammation and hyperoxia. *Proc Natl Acad Sci U S A* 110(35): 14384-14389.

Palsson-McDermott, E. M. and O'Neill, L. A. (2004). Signal transduction by the lipopolysaccharide receptor, Toll-like receptor-4. *Immunology* 113(2): 153-162.

Parker, T. A. and Abman, S. H. (2003). The pulmonary circulation in bronchopulmonary dysplasia. *Semin Neonatol* 8(1): 51-61.

Pellegrino, R., Viegi, G., Brusasco, V., Crapo, R. O., Burgos, F., Casaburi, R., Coates, A., van der Grinten, C. P., Gustafsson, P., Hankinson, J., et al. (2005). Interpretative strategies for lung function tests. *Eur Respir J* 26(5): 948-968.

Risling, T. E., Caulkett, N. A. and Florence, D. (2012). Open-drop anesthesia for small laboratory animals. *Can Vet J* 53(3): 299-302.

Royce, S. G., Nold, M. F., Bui, C., Donovan, C., Lam, M., Lamanna, E., Rudloff, I., Bourke, J. E. and Nold-Petry, C. A. (2016). Airway Remodeling and Hyperreactivity in a Model of Bronchopulmonary Dysplasia and Their Modulation by IL-1 Receptor Antagonist. *Am J Respir Cell Mol Biol* 55(6): 858-868.

Rudloff, I., Cho, S. X., Bui, C. B., McLean, C., Veldman, A., Berger, P. J., Nold, M. F. and Nold-Petry, C. A. (2017). Refining anti-inflammatory therapy strategies for bronchopulmonary dysplasia. *J Cell Mol Med* 21(6): 1128-1138.

Sahni, M., Yeboah, B., Das, P., Shah, D., Ponnalagu, D., Singh, H., Nelin, L. D. and Bhandari, V. (2020). Novel biomarkers of bronchopulmonary dysplasia and bronchopulmonary dysplasia-associated pulmonary hypertension. *J Perinatol* 40(11): 1634-1643.

Schittny, J. C. (2017). Development of the lung. *Cell Tissue Res* 367(3): 427-444.

Sibley, C. H., Plass, N., Snow, J., Wiggs, E. A., Brewer, C. C., King, K. A., Zalewski, C., Kim, H. J., Bishop, R., Hill, S., et al. (2012). Sustained response and prevention of damage progression in patients with neonatal-onset multisystem inflammatory disease treated with anakinra: a cohort study to determine three- and five-year outcomes. *Arthritis Rheum* 64(7): 2375-2386.

Swaney, W. T., Dubose, B. N., Curley, J. P. and Champagne, F. A. (2012). Sexual experience affects reproductive behavior and preoptic androgen receptors in male mice. *Horm Behav* 61(4): 472-478.

Thebaud, B., Goss, K. N., Laughon, M., Whitsett, J. A., Abman, S. H., Steinhorn, R. H., Aschner, J. L., Davis, P. G., McGrath-Morrow, S. A., Soll, R. F., et al. (2019). Bronchopulmonary dysplasia. *Nat Rev Dis Primers* 5(1): 78.

Torres-Cuevas, I., Parra-Llorca, A., Sanchez-Illana, A., Nunez-Ramiro, A., Kuligowski, J., Chafer-Pericas, C., Cernada, M., Escobar, J. and Vento, M. (2017). Oxygen and oxidative stress in the perinatal period. *Redox Biol* 12: 674-681.

Van Der Lee, S. and Boot, L. M. (1955). Spontaneous pseudopregnancy in mice. *Acta Physiol Pharmacol Neerl* 4(3): 442-444.

Velten, M., Heyob, K. M., Rogers, L. K. and Welty, S. E. (2010). Deficits in lung alveolarization and function after systemic maternal inflammation and neonatal hyperoxia exposure. *J Appl Physiol (1985)* 108(5): 1347-1356.

Whitten, W. K. (1956). Modification of the oestrous cycle of the mouse by external stimuli associated with the male. *J Endocrinol* 13(4): 399-404.